JOURNAL OF APPLIED ELECTROCHEMISTRY 19 (1989) 394–400

Studies on nonisothermal solid state galvanic cells – effect of gradients on EMF

S. K. RAMASESHA, K. T. JACOB

Department of Metallurgy, Indian Institute of Science, Bangalore 560 012, India

Received 24 March 1988; revised 26 September 1988

An expression for the EMF of a nonisothermal galvanic cell, with gradients in both temperature and chemical potential across a solid electrolyte, is derived based on the phenomenological equations of irreversible thermodynamics. The EMF of the nonisothermal cell can be written as a sum of the contributions from the chemical potential gradient and the EMF of a thermocell operating in the same temperature gradient but at unit activity of the neutral form of the migrating species. The validity of the derived equation is confirmed experimentally by imposing nonlinear gradients of temperature and chemical potential across galvanic cells constructed using fully stabilized zirconia as the electrolyte. The nature of the gradient has no effect on the EMF.

Nomenclature

J_i	flux of species i
X_i	generalized forces
L_{ij}	Onsagar coefficient
η_1	electrochemical potential of ions
η_2	electrochemical potential of electrons
T	absolute temperature
U_1^*	total energy of transfer of the ion
$\bar{H}_1$	partial molar enthalpy of the ion
Q_1^*	heat of transport of the ion
Z_1	charge on the ion
F	Faraday constant
ϕ	electrostatic potential
μ_2	chemical potential of the electron
μ_1	chemical potential of the ion
$\bar{S}_1$	partial entropy of the ion
E_{SE}	EMF developed across the solid electrolyte
E_{Pt}	EMF developed across the platinum lead
$(\mu_2)_{Pt}$	chemical potential of electrons in platinum
$(\bar{S}_2)_{Pt}$	partial entropy of electrons in platinum
$(Q_2^*)_{Pt}$	heat of transport of electrons in platinum
E_{cell}	EMF developed across the whole cell
μ_{O_2}	chemical potential of oxygen
$\mu_{O_2}^0$	chemical potential of oxygen in its standard state
R	universal gas constant
P_{O_2}	partial pressure of oxygen
$\Delta\mu_{O_2}$	relative chemical potential of oxygen
$\Delta\mu_M$	relative chemical potential of metal M
a_M	activity of metal M

1. Introduction

Isothermal solid state galvanic sensors have been extensively used for the determination of chemical potential and concentration of oxygen in industrial melts at high temperatures [1, 2]. At temperatures in excess of 1800 K and in corrosive melts the probes function only for short periods (~ 500 s) beyond which the electrolyte and electrode materials either dissolve or partake in a chemical reaction, thus destroying the integrity of the device. Sensors now available are single reading disposable devices involving stabilized zirconia as the electrolyte.

Continuous measurements have been attempted using an electrolyte tube coated with a porous ceramic layer [3–6] or a pellet sealed in a refractory tube [7]. While the life of the probe has been marginally improved, continuous operation has not been reproducibly achieved by these methods. The inherent problem is the destruction of the solid electrolyte by the melt at the point of contact. When solid reference electrodes are used, reaction between this electrode and the solid electrolyte at high temperature can also adversely affect the performance of the probe.

A design solution to the problem of chemical reactivity consists in allowing a rod of the solid electrolyte to be gradually introduced into the melt at a rate commensurate with the rate of reaction. A new volume element of the unreacted electrolyte, continuously introduced into the melt, can function before it is destroyed by the melt. The rod may be fed horizontally through the furnace wall or vertically from the top of the melt. The rate of feed can be automatically controlled. Conductivity measurements can be used to ensure that a functioning solid electrolyte is always in contact with the melt. In this proposed 'feeder design' of the sensor the reference electrode is placed at the other end of the long rod made of the solid electrolyte, away from the melt. The temperature of the reference electrode is generally much lower than that of the melt, thus minimizing chemical interactions between the reference electrode and the electrolyte. As a consequence of the design the galvanic cell is nonisothermal. The purpose of this

0021-891X/89 $03.00 + .12

paper is to develop a theoretical equation for the EMF of a nonisothermal galvanic cell and to check its validity by EMF measurement on cells with different imposed gradients in both temperature and chemical potential.

2. Theory of nonisothermal galvanic cells

Wagner [8] has analysed the Seebeck coefficient and EMF of thermocells consisting of a solid electrolyte exposed to a temperature gradient, but at constant activity of one of the constituents of the solid electrolyte. The literature does not contain a rigorous derivation for the EMF of a galvanic cell with simultaneous presence of both temperature and chemical potential gradients.

In most ionic conductors only a single ion is mobile and under a given set of conditions concentration of one of the electronic charge carriers (either electron or hole) predominates. The phenomenological flux equations of irreversible thermodynamics can then be written as

$$J_1 = L_{11}X_1 + L_{12}X_2 + L_{13}X_3 \quad (1)$$

$$J_2 = L_{21}X_1 + L_{22}X_2 + L_{23}X_3 \quad (2)$$

$$J_3 = L_{31}X_1 + L_{32}X_2 + L_{33}X_3 \quad (3)$$

where L_{ij}s are the Onsagar coefficients relating the forces X_is with the fluxes J_is. The forces are defined so that the rate of entropy production per unit volume is equal to $\Sigma_{i=1}^{3} J_i X_i$:

$$X_1 = -\frac{\mathrm{d}}{\mathrm{d}x}\left(\frac{\eta_1}{T}\right); \quad X_2 = -\frac{\mathrm{d}}{\mathrm{d}x}\left(\frac{\eta_2}{T}\right);$$

$$X_3 = \frac{\mathrm{d}}{\mathrm{d}x}\left(\frac{1}{T}\right) = -\frac{1}{T^2}\frac{\mathrm{d}T}{\mathrm{d}x} \quad (4)$$

where η_1 and η_2 are the electrochemical potentials of ions and electrons, respectively and T is the absolute temperature. Experience shows that in ionic solids the motions of ions and electrons are independent of each other. Therefore

$$L_{12} = L_{21} = 0 \quad (5)$$

Consequently

$$J_1 = -L_{11}\frac{\mathrm{d}}{\mathrm{d}x}\left(\frac{\eta_1}{T}\right) - \frac{L_{13}}{T^2}\frac{\mathrm{d}T}{\mathrm{d}x}$$

$$= -\frac{L_{11}}{T}\frac{\mathrm{d}\eta_1}{\mathrm{d}x} + \frac{L_{11}\eta_1}{T^2}\frac{\mathrm{d}T}{\mathrm{d}x} - \frac{L_{13}}{T^2}\frac{\mathrm{d}T}{\mathrm{d}x} \quad (6)$$

In the case of a pure ionic conductor ($t_{\mathrm{ion}} = 1$), at steady state the ionic flux (J_1) under open circuit conditions is zero. Therefore

$$-\frac{\mathrm{d}\eta_1}{\mathrm{d}x} + \left(\eta_1 - \frac{L_{13}}{L_{11}}\right)\frac{1}{T}\frac{\mathrm{d}T}{\mathrm{d}x} = 0 \quad (7)$$

The ratio of heat flux to ionic flux under isothermal conditions ($\mathrm{d}T/\mathrm{d}x = 0$) and at constant electrochemical potential η_2 of the electrons, is

$$\frac{J_3}{J_1} = \frac{L_{13}}{L_{11}} = U_1^* \quad (8)$$

where U_1^* is the energy of transfer of the ion (1) and the Onsagar reciprocity relation $L_{31} = L_{13}$ has been utilized. Since U_1^* includes all forms of energy transferred by the ion, it can be written as

$$U_1^* = \bar{H}_1 + Q_1^* + Z_1F\phi \quad (9)$$

where $\bar{H}_1$ is the partial molar enthalpy and Q_1^* is the heat of transport of the ion in the solid electrolyte, Z_1 is the charge on the ion, F is the Faraday constant and ϕ is the electrostatic potential. Hence

$$\frac{L_{13}}{L_{11}} = \bar{H}_1 + Q_1^* + Z_1F\phi \quad (10)$$

Substituting this result in Equation 7 and expressing the electrochemical potential of the ion in terms of its chemical potential and the electric field contribution, $\eta_1 = \mu_1 + Z_1F\phi$, gives

$$-\frac{\mathrm{d}(\mu_1 + Z_1F\phi)}{\mathrm{d}x} + (\mu_1 - \bar{H}_1 - Q_1^*)\frac{1}{T}\frac{\mathrm{d}T}{\mathrm{d}x} = 0 \quad (11)$$

Since $\mu_1 = H_1 - TS_1$, Equation 11 can be recast as

$$-\frac{\mathrm{d}\mu_1}{\mathrm{d}x} - Z_1F\frac{\mathrm{d}\phi}{\mathrm{d}x} - \left(\bar{S}_1 + \frac{Q_1^*}{T}\right)\frac{\mathrm{d}T}{\mathrm{d}x} = 0 \quad (12)$$

where $\bar{S}_1$ is the partial entropy of the ion in the solid electrolyte. Integrating the expression between the limits x' and x'' which mark the extremities of the solid electrolyte where the chemical potential and temperature are μ_1', T' and μ_1'', T'', respectively, one obtains

$$-Z_1FE_{\mathrm{SE}} = (\mu_1'' - \mu_1') + \bar{S}_1(T'' - T') + Q_1^* \ln\frac{T''}{T'} \quad (13)$$

where $E_{\mathrm{SE}} = (\phi'' - \phi')_{\mathrm{SE}}$ is the EMF developed across the ends of the solid electrolyte. For EMF measurements the solid electrolyte must be connected by an electric lead to an instrument. Platinum is frequently used as leads in galvanic sensors. Following the same procedure as for the ionic conductor, the thermo-EMF developed in the platinum lead is given by

$$FE_{\mathrm{Pt}} = (\phi'' - \phi')_{\mathrm{Pt}} = (\mu_2'' - \mu_2')_{\mathrm{Pt}} + (\bar{S}_2)_{\mathrm{Pt}}(T'' - T') + (Q_2^*)_{\mathrm{Pt}} \ln\frac{T''}{T'} \quad (14)$$

where $(\bar{S}_2)_{\mathrm{Pt}}$ and $(Q_2^*)_{\mathrm{Pt}}$ are the partial entropy and heat of transport of electrons in platinum. The cell EMF is the difference between the EMF developed across the solid electrolyte and the platinum lead

$$E_{\mathrm{cell}} = E_{\mathrm{SE}} - E_{\mathrm{Pt}} = -\frac{1}{Z_1F}(\mu_1'' - \mu_1')_{\mathrm{SE}} - \frac{1}{Z_1F}\left[\bar{S}_1(T'' - T') + Q_1^* \ln\frac{T''}{T'}\right]_{\mathrm{SE}} - \frac{1}{F}(\mu_2'' - \mu_2') - \frac{1}{F}\left[\bar{S}_2(T'' - T') + Q_2^* \ln\frac{T''}{T'}\right]_{\mathrm{Pt}} \quad (15)$$

Assuming local equilibrium at the electrode/electrolyte interface, the electrochemical potentials of electrons in platinum and the solid electrolyte at each terminal is the same. For an oxygen ion conductor $Z_1 = -2$ and the reaction at each electrode is

$$\tfrac{1}{2}O_2 + 2e \longrightarrow O^{2-} \tag{16}$$

Therefore

$$\tfrac{1}{2}\mu_{O_2} = \mu_1 - 2\mu_2 \tag{17}$$

Combining Equations 15 and 17

$$E_{cell} = \frac{1}{4F}(\mu''_{O_2} - \mu'_{O_2}) + \frac{1}{2F}\left[\bar{S}_1(T'' - T') + Q_1^* \ln \frac{T''}{T'}\right]_{SE} - \frac{1}{F}\left[\bar{S}_2(T'' - T') + Q_2^* \ln \frac{T''}{T'}\right]_{Pt} \tag{18}$$

The chemical potential of oxygen can be expressed as the sum of the chemical potential in its standard state (at 1 atm pressure) and its relative chemical potential

$$\mu_{O_2} = \mu^0_{O_2} + RT \ln P_{O_2} = \mu^0_{O_2} + \Delta\mu_{O_2} \tag{19}$$

Substituting for μ_{O_2} in Equation 18

$$E_{cell} = \frac{1}{4F}(\Delta\mu''_{O_2} - \Delta\mu'_{O_2}) + \frac{1}{4F}(\mu^{0\prime\prime}_{O_2} - \mu^{0\prime}_{O_2}) + \frac{1}{2F}\left[\bar{S}_1(T'' - T') + Q_1^* \ln \frac{T''}{T'}\right]_{SE} - \frac{1}{F}\left[\bar{S}_2(T'' - T') + Q_2^* \ln \frac{T''}{T'}\right]_{Pt} \tag{20}$$

This is the fundamental equation for the EMF of a nonisothermal galvanic cell. However, it contains terms such as $\bar{S}_i$, the partial entropy of charged species, and Q_i^*, the heat of transport, which are not amenable to direct measurement or calculation. To overcome this problem, the EMF of a thermocell in pure oxygen at 1 atm pressure can be measured. The first term on the right side of Equation 20 is now zero since $P_{O_2} = 1$ at both electrodes.

$$E_{thermocell} = \frac{1}{4F}(\mu^{0\prime\prime}_{O_2} - \mu^{0\prime}_{O_2}) + \frac{1}{2F}\left[\bar{S}_1(T'' - T') + Q_1^* \ln \frac{T''}{T'}\right]_{SE} - \frac{1}{F}\left[\bar{S}_2(T'' - T') + Q_2^* \ln \frac{T''}{T'}\right]_{Pt} \tag{21}$$

The EMF of the nonisothermal cell can therefore be expressed as the EMF of a thermocell operating under pure oxygen at 1 atm pressure in the same temperature gradient and a contribution arising from the chemical potential difference between the two electrodes.

$$E_{cell} = E^{\text{pure } O_2}_{\text{thermocell}} + \frac{1}{4F}(\Delta\mu''_{O_2} - \Delta\mu'_{O_2}) = E^{\text{pure } O_2}_{\text{thermocell}} + \frac{R}{4F}(T'' \ln P''_{O_2} - T' \ln P'_{O_2}) \tag{22}$$

This is the most practical expression for the EMF of a nonisothermal galvanic cell. It is readily seen that when $T' = T''$ (i.e. for an isothermal cell), the first term on the right of Equation 20 is zero and the cell EMF reduces to the familiar Nernst equation

$$E_{cell} = \frac{RT}{4F} \ln (P''_{O_2}/P'_{O_2}) \tag{23}$$

Similarly for a solid electrolyte in which the cation is the migrating species, the EMF of a nonisothermal cell is given by

$$E_{cell} = E^{\text{pure M}}_{\text{thermocell}} - \frac{1}{Z_1 F}(\Delta\mu''_M - \Delta\mu'_M) \tag{24}$$

where $E_{thermocell}$ is the EMF of a thermocell operating in the same temperature gradient as the nonisothermal galvanic cell, but with the metal M at unit activity at each electrode. The term $\Delta\mu_M$ is equal to $RT \ln a_M$.

3. Experimental details

3.1. *Scope*

The experiments were designed to verify the equation for the EMF of a nonisothermal cell using calcia-stabilized zirconia as the solid electrolyte. The oxygen potential at the high temperature electrode was established by mixture of Ni and NiO. At the low-temperature electrode the oxygen partial pressure is determined by the dissociation of Cu_2O to Cu. In this configuration the oxygen potential in the solid electrolyte at steady state decreases monotonically with distance from the Ni + NiO electrode towards the Cu + Cu_2O electrode. The presence of a maximum or minimum in temperature and chemical potential variation across the solid electrolyte provides a more rigorous test for the applicability of the equation. An extremum in oxygen potential was induced by placing a mixture of either Co + CoO, Fe + FeO or Cr + Cr_2O_3 in contact with the solid electrolyte in between the terminal electrodes. By using three independent heating coils, different types of temperature gradients were imposed on the solid electrolyte. The Seebeck coefficient of the cell with calcia-stabilized zirconia in pure oxygen at a pressure of 1.01×10^5 Pa was redetermined as a function of temperature, since this information is basic to the calculation of the EMF of a nonisothermal cell.

3.2. *Materials*

Fine powders of Cu, Ni, Co, Fe, Cr and their oxides Cu_2O, NiO, CoO, Fe_2O_3 and Cr_2O_3 of specpure grade were supplied by Johnson Matthey Chemicals. Alumina powder of 99.8% purity was obtained from Cerac Inc. Calcia-stabilized zirconia rods, 3 mm in diameter and 150 mm in length, contained 15 mol % CaO. The argon gas used to provide an inert atmosphere over the cell was 99.99% pure and was further dried with magnesium perchlorate and deoxidized by

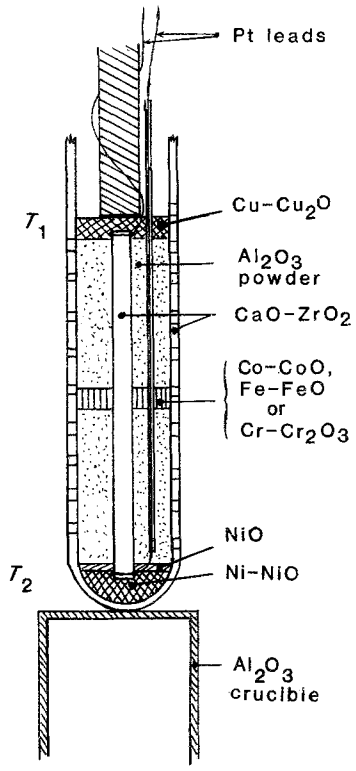

Fig. 1. Schematic cell assembly used in EMF measurements.

passing over copper at 700 K and titanium granules at 1150 K.

3.3. *Apparatus and procedure*

A schematic diagram of the cell assembly is shown in Fig. 1. An intimate mixture of Ni and NiO powders in the molar ratio 2 : 1 was taken in a closed-end alumina tube 18 mm in diameter. Small grooves were cut around each end of the calcia-stabilized zirconia rod and separate Pt/Pt-13% Rh thermocouples were attached to each end. One end of the zirconia rod with the attached thermocouple was buried in the Ni + NiO mixture. The thermocouple leads passed through a twin bore thermocouple sheath. A layer of pure NiO was placed over the Ni + NiO mixture and the alumina tube was then filled tightly with dry alumina powder to a height of ~65 mm. A presintered pellet of either Co + CoO, Fe + FeO or Cr + Cr_2O_3, with holes for the zirconia rod and thermocouple sheath, was placed on top of the column of alumina powder. The space between the presintered pellet and the tubes was packed with the same material as the pellet. The molar ratio of metal to oxide in the pellet was 2 : 1. The Fe + FeO pellet was prepared from fine powders of Fe and Fe_2O_3 in the appropriate ratio followed by heat treatment at 1300 K under argon. Alumina powder was again tightly packed above the sintered pellet for ~65 mm. A mixture of Cu + Cu_2O was packed around the top end of the zirconia rod. A circular presintered pellet of Cu + Cu_2O, provided with a hole for the thermocouple, was placed above the zirconia rod and the packed column was pressed down by a spring-loaded alumina rod.

The entire assembly was suspended in an outer alumina tube placed in a vertical three-zone furnace. At the beginning of each experiment the outer alumina tube was evacuated and filled with prepurified argon gas. Slits in the closed-end alumina tube, containing the zirconia rod and electrodes, permitted entrapped air and desorbed gases to escape. An argon flow rate of 5 ml s^{-1} was maintained through the outer tube during the experiment. Argon gas was also passed over the Ni + NiO and Cu + Cu_2O electrodes at a rate of 0.3 ml s^{-1} via the thermocouple sheaths.

By independent control of the three separate heating zones of the furnace it was possible to generate different temperature profiles in the furnace. The Ni + NiO electrode was held in the main constant temperature (± 1 K) zone of the furnace. The Cu + Cu_2O electrode was positioned in a smaller secondary constant temperature (± 1.5 K) zone. In the

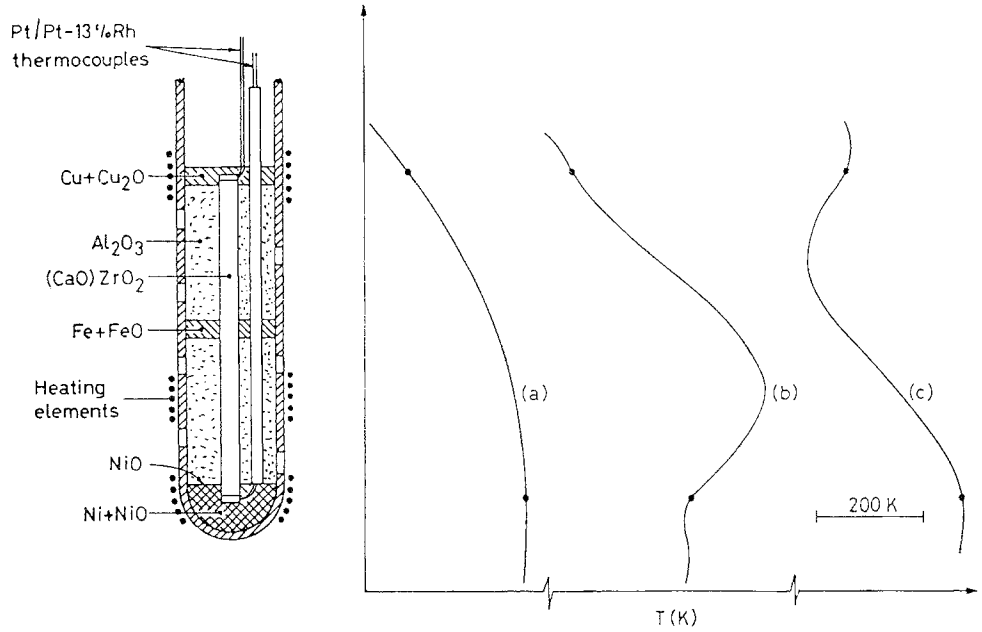

Fig. 2. The three temperature gradients used across the solid electrolyte.

Table 1. The reversible EMF of the cells I, II and III with monotonic temperature variation

$X + XO$	$T'(K)$	$T''(K)$	$E\ (mV)$ measured	$E\ (mV)$ calculated
	1264	1373	254 (±2)	255.1
Co + CoO	1171	1273	265 (±4)	262.0
	1079	1173	268 (±5)	268.8
	1265	1373	255 (±2)	255.1
Fe + FeO	1170	1273	259 (±4)	262.1
	1078	1173	269 (±4)	268.9
	1263	1373	253 (±2)	255.2
$Cr + Cr_2O_3$	1169	1273	259 (±5)	262.1
	1078	1173	265 (±5)	268.9

first set of experiments the EMFs of the following cell were measured at different temperatures using a high-impedance ($> 10^{12}\ \Omega$) digital voltmeter:

$$\text{Pt, Cu} + \text{Cu}_2\text{O}\ (T')\ \|\ (\text{CaO})\ \text{ZrO}_2\ \|\ \text{Co} + \text{CoO}\ \|\ (\text{CaO})\ \text{ZrO}_2\ \|\ (T'')\ \text{Ni} + \text{NiO, Pt} \quad \text{(I)}$$

$$\text{Pt, Cu} + \text{Cu}_2\text{O}\ (T')\ \|\ (\text{CaO})\ \text{ZrO}_2\ \|\ \text{Fe} + \text{FeO}\ \|\ (\text{CaO})\ \text{ZrO}_2\ \|\ (T'')\ \text{Ni} + \text{NiO, Pt} \quad \text{(II)}$$

$$\text{Pt, Cu} + \text{Cu}_2\text{O}\ (T')\ \|\ (\text{CaO})\ \text{ZrO}_2\ \|\ \text{Cr} + \text{Cr}_2\text{O}_3\ \|\ (\text{CaO})\ \text{ZrO}_2\ \|\ (T'')\ \text{Ni} + \text{NiO, Pt} \quad \text{(III)}$$

In this set of experiments the temperature decreased montonically from the right-hand electrode to the left-hand electrode. The cells were characterized by gradients in both temperature and chemical potential of oxygen, with the latter exhibiting an extremum approximately mid-way through the solid electrolyte. The outer alumina tube enclosing the cell assembly was surrounded by an earthed stainless steel sheet to avoid induced EMF on the platinum leads from the furnace winding. The cell EMF was not sensitive to variations in the flow rate of argon gas by a factor of two. The reversibility of the EMF was checked by passing small currents ($\sim 50\ \mu A$) through the cell for 100 s. In each case the EMF returned to the steady value before the coulometric titration in approximately 1.2 ks.

In a second set of experiments the temperature profile across the solid electrolyte was altered as shown in Fig. 2 by inserting three separate heating elements around the closed-end alumina tube. The EMFs of the three cells were again measured for each type of temperature profile shown in Fig. 2. Steady EMFs were generally obtained in approximately 3 ks after steady state thermal profiles were established. In a third set of experiments the Seebeck coefficient of the cell with fully stabilized zirconia solid electrolyte containing 15 mol % CaO in pure oxygen at a pressure of 1.01×10^5 Pa was measured using an arrangement similar to that described earlier [9] in the temperature range 1100–1800 K. A horizontal resistance furnace with molybdenum heating element was used.

4. Results

The reversible EMFs of cells I, II and III obtained in the first set of experiments are summarized in Table 1 along with the corresponding temperatures of the terminal electrodes. The reproducibility of the EMF improves with the average temperature of the cell. Generally the EMF is monitored for periods in excess of 30 ks. The uncertainty limits correspond to twice the standard deviation. When long rods of stabilized zirconia are used in the construction of nonisothermal sensors, satisfactory reproducibility and response time cannot be obtained when the lower temperature electrode is maintained below 1000 K.

The cell EMFs obtained with extreme temperature profiles are given in Table 2. It is clear that the nature of the temperature profile between the terminal electrodes does not significantly affect the EMF of the nonisothermal cell. This is in conformity with the theory outlined in Section 2. The response time of the cell is shorter by approximately 30% when the temperature profiles with a maximum or a minimum are imposed on the cell.

The function $\psi^{\text{pure O}_2} = E^{\text{pure O}_2}_{\text{thermocell}}/(T'' - T')$ for the thermocell using fully stabilized zirconia containing 15 mol % CaO is plotted in Fig. 3 as a function of the mean temperature of the solid electrolyte. Temperature differences of ~ 100 K across the terminals of a zirconia rod are imposed in pure oxygen gas at a pressure of 1.01×10^5 Pa and flowing at 2 ml s^{-1} over

Table 2. EMF of nonisothermal cells I, II and III exposed to different types of temperature profile

Type of temperature profile	$X + XO$	$T'(K)$	$T''(K)$	$E\ (mV)$ measured	$E\ (mV)$ calculated
a	Co + CoO	1160	1372	262 (±3)	260.6
b	Co + CoO	1189	1368	260 (±3)	259.1
c	Co + CoO	1142	1374	262 (±3)	261.5
a	Fe + FeO	1158	1373	258 (±3)	260.6
b	Fe + FeO	1190	1370	257 (±3)	260.0
c	Fe + FeO	1140	1373	259 (±3)	261.6
a	$Cr + Cr_2O_3$	1157	1370	257 (±3)	260.8
b	$Cr + Cr_2O_3$	1192	1366	256 (±3)	259.0
c	$Cr + Cr_2O_3$	1141	1375	258 (±4)	261.5

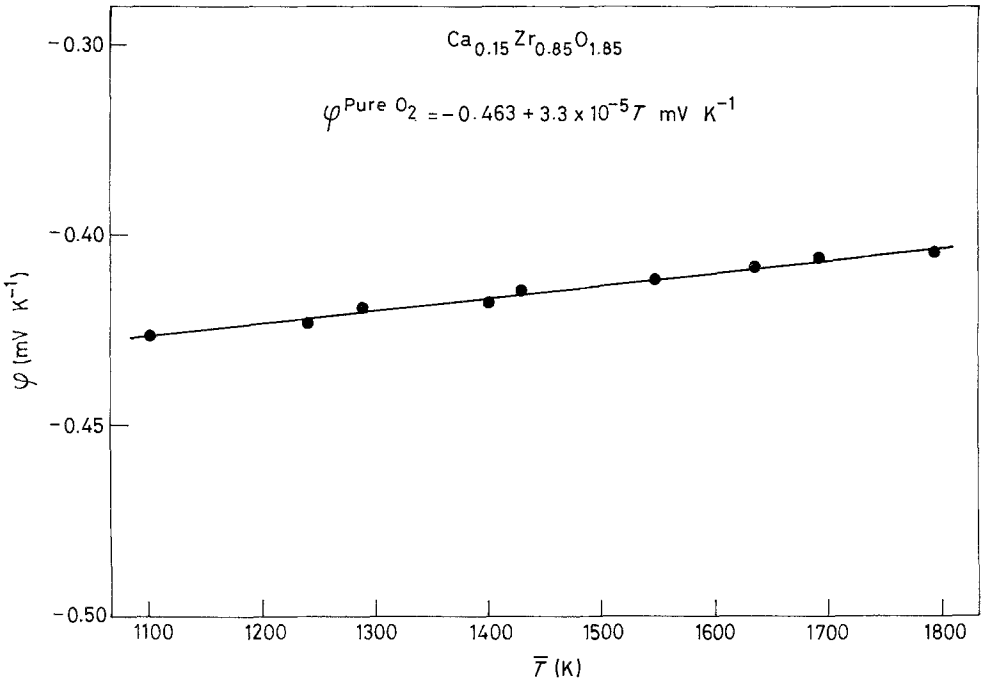

Fig. 3. ψ of a thermocell using calcia-stabilized zirconia as a function of average temperature $\bar{T}$ as pure oxygen at 1.01 × 10^5 Pa.

both electrodes. The direction of gas flow and flow rate had no effect on $\psi^{\text{pure}\,O_2}$. The function $\psi^{\text{pure}\,O_2}$ shows only a slight temperature dependence. The least mean squares regression analysis gives the expression

$$\psi^{\text{pure}\,O_2} = \frac{E^{\text{pure}\,O_2}_{\text{thermocell}}}{(T'' - T')}$$

$$= -0.463 + 3.3 \times 10^{-5}\,\bar{T}(\text{K})\,\text{mV K}^{-1} \quad (25)$$

The value of $\psi^{\text{pure}\,O_2}$ is determined by the Seebeck coefficients of both the solid electrolyte and platinum, the latter being almost negligible compared to the former.

5. Discussion

The measurement EMF of the nonisothermal cells I, II and III can be compared with values computed using Equation 22. The variation of the relative chemical potential of oxygen in Ni + NiO and Cu + Cu_2O electrodes as a function of temperature are well established [10, 11]

$$\Delta\mu_{O_2}(\text{Ni} + \text{NiO}) = -468\,320 + 169.79\,T\,\text{J mol}^{-1} \quad (26)$$

$$\Delta\mu_{O_2}(\text{Cu} + \text{Cu}_2\text{O}) = -335\,380 + 143.20\,T\,\text{J mol}^{-1} \quad (27)$$

The values of the EMF of the thermocell in pure oxygen can be computed from Equation 25. The computed EMFs are listed in Tables 1 and 2 for comparison. There is good agrement with experiment. The fluctuations in EMF of nonisothermal cells are approximately three times the corresponding value for isothermal cells. This is at least in part due to small temperature gradients present at the terminal electrodes of the nonisothermal cells used in this study and to the slightly larger fluctuation in temperature (± 2 K) compared to isothermal cells placed in a larger even temperature zone of the furnace.

The results obtained in this study clearly establish the validity of the expression for the EMF of a galvanic cell exposed to coupled gradients in chemical potential and temperature obtained from the phenomenological equations of irreversible thermodynamics. The two approximations used in the derivation of the expression for EMF – $L_{12} = L_{21} = 0$ and constant values for Q_i^* and $\bar{S}_i$ independent of temperature and chemical potential – are clearly validated by experimental data. These approximations are generally used in the analyses of transport phenomena in predominantly ionic conductors [8]. It is anticipated that nonisothermal sensors will find many useful applications in process control at elevated temperatures and in corrosive environments where chemical reactivity and mutual solubility limit the life time of conventional isothermal solid state devices.

Acknowledgement

The authors are grateful to Ms R. Sarojini for the assistance in preparation of the manuscript.

References

[1] D. Janke, in 'Science and Technology of Zirconia II' (edited by N. Claussen, M. Rühle and A. H. Heuer), Advances of Ceramics, Vol. 12, Am. Ceram. Soc., Ohio, USA (1984) p. 636.
[2] K. S. Goto, *Trans. Iron Steel Inst. Japan* **16** (1976) 469.
[3] C. Gatellier and M. Olette, *Compt. Rend.* **226C** (1968) 1133.
[4] K. H. Ulrich and K. Borowski, *Arch. Eisenhüttenwes* **39** (1968) 259.
[5] W. A. Fischer and D. Janke, *Arch. Eisenhüttenwes* **42** (1971) 249.
[6] S. M. Shveikin, B. A. Kamaev, N. F. Bakhcheev, G. P.

Zakharov and V. A. Kovylin, *Steel in the USSR* **3** (1973) 905.
[7] E. Forster and H. Richter, *Arch. Eisenhüttenwes* **40** (1969) 475.
[8] C. Wagner, *Prog. Solid State Chem* **7** (1972) 1.
[9] C. B. Alcock, K. Fitzner and K. T. Jacob, *J. Chem. Thermodyn.* **9** (1977) 1011.
[10] B. C. H. Steele, in 'Electromotive Force Measurements in High Temperature Systems' (edited by C. B. Alcock), Inst. Min. Met., London (1968) 3.
[11] K. T. Jacob and J. H. E. Jeffes, *Trans. Inst. Min. Met.* **80C** (1971) C32.